Characterization of *Chlorobium tepidum* Chlorosomes: A Calculation of Bacteriochlorophyll *c* per Chlorosome and Oligomer Modeling

Gabriel A. Montaño,* Benjamin P. Bowen,† Jeffrey T. LaBelle,‡ Neal W. Woodbury,* Vincent B. Pizziconi,‡ and Robert E. Blankenship*

*Department of Chemistry and Biochemistry, †Department of Chemical and Materials Engineering, and ‡Department of Bioengineering, Arizona State University, Tempe, Arizona 85287-1604 USA

ABSTRACT The bacteriochlorophyll (Bchl) *c* content and organization was determined for *Chlorobium* (*Cb.*) *tepidum* chlorosomes, the light-harvesting complexes from green photosynthetic bacteria, using fluorescence correlation spectroscopy and atomic force microscopy. Single-chlorosome fluorescence data was analyzed in terms of the correlation of the fluorescence intensity with time. Using this technique, known as fluorescence correlation spectroscopy, chlorosomes were shown to have a hydrodynamic radius (Rh) of 25 ± 3.2 nm. This technique was also used to determine the concentration of chlorosomes in a sample, and pigment extraction and quantitation was used to determine the molar concentration of Bchl *c* present. From these data, a number of ~215,000 ± 80,000 Bchl *c* per chlorosome was determined. Homogeneity of the sample was further characterized by dynamic light scattering, giving a single population of particles with a hydrodynamic radius of 26.8 ± 3.7 nm in the sample. Tapping-mode atomic force microscopy (TMAFM) was used to determine the *x,y,z* dimensions of chlorosomes present in the sample. The results of the TMAFM studies indicated that the average chlorosome dimensions for *Cb. tepidum* was 174 ± 8.3 × 91.4 ± 7.7 × 10.9 ± 2.71 nm and an overall average volume 90,800 nm^3 for the chlorosomes was determined. The data collected from these experiments as well as a model for Bchl *c* aggregate dimensions was used to determine possible arrangements of Bchl *c* oligomers in the chlorosomes. The results obtained in this study have significant implications on chlorosome structure and architecture, and will allow a more thorough investigation of the energetics of photosynthetic light harvesting in green bacteria.

INTRODUCTION

Green bacteria contain complexes known as chlorosomes as their main light-harvesting complex, but unlike most light-harvesting complexes, proteins are of secondary importance in determining pigment geometry in the chlorosome (Blankenship et al., 1995; Griebenow and Holzwarth, 1989; Prokhorenko et al., 2000). Chlorosomes utilize a pigment-pigment architecture instead of pigment-protein scaffolding to create large oligomers that fill the interior of the chlorosome (Blankenship et al., 1995; Brune et al., 1987; Griebenow and Holzwarth, 1989). Along the base of the chlorosome is a pigment-protein complex known as the baseplate. It serves as an intermediate in energy transfer to the reaction center. On the periphery of the membrane between the baseplate of the chlorosome and the reaction center is the Fenna-Matthews-Olson (FMO) complex. The FMO complex is found only in green sulfur bacteria. It is a trimeric light-harvesting complex that serves as an intermediary in energy transfer from the baseplate complex of the chlorosome to the reaction center (Blankenship et al., 1995).

Chlorosomes, found only in green photosynthetic bacteria, are large supramolecular sac-like complexes that are attached to the cytoplasmic side of the inner cell membrane. Chlorosomes were first observed by Cohen-Bazire et al. (1964) when they noted the presence of oblong inclusion bodies along the inner cell membrane in thin sections of *Chlorobium limicola* and *Chlorobium thiosulfatophilum*.

Chlorosomes are oblong structures that range in size depending on the species. *Chloroflexus* (*Cf.*) *aurantiacus* chlorosomes have an average length of 106 ± 24 nm, a width of 32 ± 10 nm, and a height of 10–20 nm (Oelze and Golecki, 1995). In general, *Chlorobium*-type chlorosomes are larger than those of *Cf. aurantiacus*. *Cb. tepidum* chlorosomes have been reported to have lengths ranging 100–180 nm, widths ranging 40–60 nm, and heights similar to the *Cf. aurantiacus* chlorosomes (Wahlund et al., 1991). However, a recent study using atomic force microscopy reported *Cf. aurantiacus* and *Cb. tepidum* chlorosomes to be of a similar size (Martinez-Planells et al., 2002). Growth studies have also found chlorosome size to have a strong dependence on light intensity and other growth conditions (Oelze and Golecki, 1995).

The chlorosome outer membrane is composed of glycolipids. Monogalactosyl diglyceride is the major lipid component of all chlorosomes and creates a surface monolayer of ~10 Å thick (Staehelin et al., 1978). This arrangement creates a very hydrophobic environment with the fatty acid tails of the lipids sticking toward the interior of the chlorosome.

The interior of the chlorosome is filled with closely packed rod-shaped structures known as rod elements. The rod elements are oriented parallel to the cytoplasmic membrane and extend the full length of the chlorosome (Staehelin et al., 1980). The sizes of the rod elements vary depending on species type. In *Cb. tepidum*, rod elements have a diameter of ~10 nm whereas in *Cf. aurantiacus*, a diameter of ~5 nm has been reported (Sprague and Staehelin, 1984; Staehelin et al., 1980).

Submitted March 11, 2003, and accepted for publication June 30, 2003.

Address reprint requests to Robert E. Blankenship, E-mail: blankenship@asu.edu.

0006-3495/03/10/2560/06 $2.00

Chlorosomes are also known to contain carotenoids, however the location of the carotenoids is unknown. Some studies have suggested the carotenoids are closely associated with the rod elements whereas others have suggested they are closely associated with the baseplate complex (Arellano et al., 2000). *Chlorobium* chlorosomes are also known to contain quinones, however their location within the chlorosome remains unknown (Frigaard et al., 1997).

All chlorosomes contain either Bchl *c, d*, or *e* or combinations of them as their major pigments. These bacteriochlorophyll species have unique characteristics that allow them to coordinate to form the rod elements. In particular, at the 3^1 position, a hydroxyl group is present and the 13^1 position lacks a bulky carboxymethyl substituent that is found in most (bacterio)chlorophylls. These two features allow for the coordination of the Mg center necessary for forming the rod elements.

Aggregation of Bchl *c* in rod elements has been studied both by in vitro aggregation of chlorosomal clorophylls and theoretical model studies. Although there is no detailed molecular structure of the chlorosomal rod elements, it is widely accepted that the Bchl *c, d*, or *e* are organized in an aggregated state in vivo, forming the rod elements with proteins playing little or no direct role.

Several rod element models have been proposed over the years (Matsuura et al., 1993; Nozawa et al., 1992a,b), including recent models that have been proposed based on computer molecular modeling and exciton dynamics interpretation (Holzwarth and Schaffner, 1994; Prokhorenko et al., 2000). The Holzwarth models are generally considered the best models proposed and are used in the model interpretation studies herein.

The number of Bchl pigments in each chlorosome was estimated to be ~10,000 by Olson et al. (1998) and this number has been widely cited. However, there has never been a direct experimental determination of this quantity.

The focus of this study was to directly determine the amount of Bchl *c* in a typical chlorosome. Chlorosomes from *Cb. tepidum* were isolated and examined using fluorescence correlation spectroscopy (FCS), dynamic light scattering (DLS) tapping mode atomic force microscopy (TMAFM), and biochemical pigment analysis. Results have been interpreted according to existing models of Bchl *c* aggregation.

MATERIALS AND METHODS

Cb. tepidum was grown phototrophically at 40°C. The cells were harvested by centrifugation at 10,000 × *g* for 10 min after 3–4 days of growth and used immediately. Chlorosomes were then isolated by a modification of the method described by Feick and Fuller (1984). Briefly, *Cb. tepidum* cells were resuspended in 0.13% miranol: 10mM Tris-HCl: 10mM ascorbic acid, homogenized, and broken in a French press operated at 20,000 psi. The disrupted membranes and cell debris were then pelleted by centrifugation at 12,500 × *g* for 20 min. The remaining supernatant liquid was then loaded onto 10–40% sucrose gradients containing 0.13% miranol. The sucrose gradients were centrifuged at 266,000 × *g* for 18 h and the chlorosomes collected from a band in the gradient located between 25% and 30% sucrose. Sucrose gradients were repeated for further purification. Isolated chlorosomes were then dialyzed in 10mM Tris-HCL buffer pH 8.0 containing 0.13% miranol.

Pigment extractions were performed by adding a small volume of isolated chlorosome sample to methanol and absorbance spectra taken immediately. Absorbance spectra were taken using a Shimadzu UV-2501PC spectrophotometer with a 2-nm spectral bandwidth. Bchl *c* absorbance (optical density $(OD)_{670}$ ~0.2) was monitored at 670 nm and an extinction coefficient of 74 mM^{-1} was used for calculation of concentrations (Feick et al., 1982).

DLS studies were performed using the DynaPro MS/X (Protein Solutions, Charlottesville, VA). Analysis was performed utilizing the program DYNAMICS V6, and all experiments were run at an operating temperature of 25°C. All DLS samples were first prepared by filtering 20 μl of chlorosome solution, obtained from the second sucrose gradient ultracentrifugation step, and using a syringe filter assembly containing a 4-μm filter with the subsequent purified sample placed into a quartz cuvette. The DLS instrument was run at a 10% laser intensity at 824.8 nm 50 mW. Sampling rate was set at two acquisitions per second, and a sample set of >20 acquisitions. Raw data was filtered to remove ''dust events'' by ignoring data with sum-of-squares error fluctuation >50%. A polydisperse model was used to determine a hydrodynamic radius (R_h) with a single population giving rise to 95.6% (by mass) of the sample.

For the fluorescence correlation spectroscopy experiments, a frequency doubled, pulse compressed, and mode locked Nd:YAG laser (532 nm, 10 ps) was used to excite the sample at a repetition rate of 82 MHz. To ensure proper beam quality and polarization, the light was passed through a single mode, polarization preserving glass fiber (F-SPA, Newport, Irvine, CA) and a polarizing beam splitter (05BC15PH.3, Newport). The laser light was delivered into an inverted, confocal microscope and reflected up toward the microscope objective with a dichroic mirror (Q570LP, Omega Optical, Brattleboro, VT). The sample, a 50-μl droplet, was placed onto a glass coverslip (22 × 50 mm No 1.5, VWR, West Chester, PA). The same objective (100× PlanApo 1.4NA, Olympus, Tokyo, Japan) used to focus the laser also collected the fluorescence. The collected fluorescence passed through the dichroic mirror and was focused onto a 50-μm diameter pinhole (910-PH50, Newport). A 720-nm longpass filter was used to separate fluorescence resulting from chlorosome excitation from scattered light. The fluorescence was then split by a polarizing beam splitter (05FC16PB.3, Newport) sending photons polarized parallel to the laser to detector one (Perkin Elmer, SPCM-AQR-12, Canada) and photons polarized perpendicular to the laser to detector two. The signal from the parallel detector was sent to a digital correlator (Flex2K-12×2, correlator.com, USA) that reports the fluorescence autocorrelation function to the computer. Analysis of the fluorescence correlation data was done according to methods previously described in the literature (Fries et al., 1998). A more detailed description of fluorescence correlation spectroscopy techniques can be found in many other works and will not be described here (Ehrenber and Rigler, 1974; Magde et al., 1972).

Tapping-mode AFM was performed using a commercial multimode AFM (Nanoscope III, Digital Instruments, Santa Barbara, CA) under ambient conditions. A stiff 125-μm silicon cantilever was used to obtain TMAFM images in both height and amplitude modes. Two chlorosome samples of $OD_{750} = 0.02$ were aliquoted on cleaved mica surfaces and allowed to air dry before imaging. Both samples were imaged with the same AFM tip. To estimate the volume of the chlorosomes, all objects observed by AFM were treated as ellipsoids and the volume calculated by $V = 4/3\pi(abc)$, where a, b, and c are the elliptical radii corresponding to the length, width, and height of the chlorosome.

RESULTS

Fluorescence correlation spectroscopy

Using fluorescence correlation spectroscopy, the concentration of chlorosomes in a sample of OD_{750} ~43 was found to be $2.6 \times 10^{-9} \pm 1.2 \times 10^{-9}$ M. The model shown below

(Eq. 1) accounts for the correlation of fluorescent events in terms of their diffusivity (D), the average number of molecules in the probe volume (N), the ratio of background intensity to signal intensity (I_b/I_s), and the dimensions of the probe volume (Zander et al., 1996).

$$G(t_c) = \frac{1}{N\sqrt{8}}\left(1 - \frac{I_b}{I_s}\right)^2 \left(\frac{1}{1 + \frac{4Dt_c}{\omega_o^2}}\right)\left(\frac{1}{1 + \frac{4Dt_c}{z_o^2}}\right)^{1/2} + 1. \quad (1)$$

Calibration of the probe volume was performed multiple times with solutions of rhodamine-6G or fluorescent microspheres from Molecular Probes (Eugene, OR). For each calibration measurement, the concentration and hydrodynamic radius of the fluorescent species was known. From these measurements for the probe volume, an average value and uncertainty in the dimensions describing the probe volume was determined (Rigler et al., 1993). A probe volume of 1.6 ± 0.75 femtoliters was measured for this system having $1/e^2$ radius $\omega_o = 330 \pm 0.20$ nm and a vertical dimension of $zo = 7.6 \pm 2.6$ μm and inserted into the equation above. The FCS curve in Fig. 1 was fit using the autocorrelation curve for a monodisperse sample (Eq. 1) and the values of ω_o and zo determined above. A hydrodynamic radius of 25.2 ± 3.2 nm was calculated from the diffusivity according to the Stokes Einstein equation. The data in Fig. 1 fits well to Eq. 1, indicating a monodisperse sample population. Results of the FCS analysis are given in Table 1.

Dynamic light scattering

Dynamic light scattering was performed on the same chlorosome sample to determine the homogeneity of the sample by a different method. DLS does not depend on the fluorescent properties of the sample, therefore it reports on the diffusive properties of all particles present in the sample. As was the case for FCS, DLS found the sample to be dominated by particles with a hydrodynamic radius of 26.8 ± 3.7 nm (Fig. 2 *b*). DLS gives a similar correlation function to that observed using FCS again indicating a monodisperse population (Fig. 2 *a*).

Tapping mode atomic force microscopy

To determine the actual size of the chlorosomes being detected, tapping mode AFM was used. Fig. 3 is a representative TMAFM image of two chlorosomes adhered to the mica surface. Fig. 3 *a* shows a top view of the chlorosomes having an ellipsoidal shape with a length of ~180 nm and a width of ~90 nm. Fig. 3 *b* shows a surface plot of the chlorosomes and gives a chlorosome thickness of ~10 nm. Section analysis found the average size of the chlorosomes to be 174 × 91.4 × 10.86 nm based upon the measurement of 10 chlorosomes (Table 2). These chlorosomes have a length and width larger than most sizes reported for *Cb. tepidum* chlorosomes, although the height is about half the size previously reported (Wahlund et al., 1991). From the dimensions measured, an average volume of 90,800 nm^3 can be calculated for the chlorosomes studied here. This volume and these dimensions can be applied to discussion of pigment organization and will be discussed later.

Chlorosome pigment quantitation

Using a sample of chlorosomes with OD_{750} ~43, the concentration of Bchl *c* was determined to be $5.7 \times 10^{-4} \pm 7.0 \times 10^{-5}$ M. Using the numbers obtained for chlorosome and Bchl *c* concentration, *Cb. tepidum* chlorosomes were

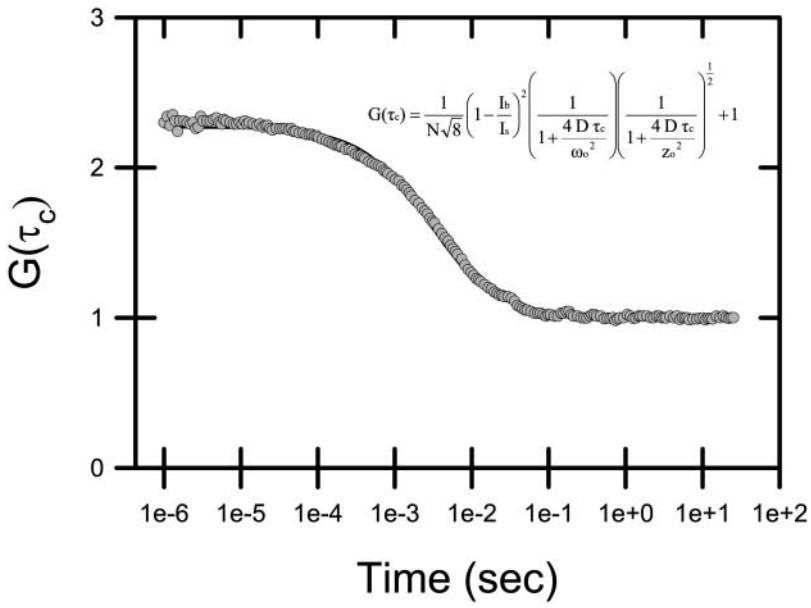

FIGURE 1 Fluorescence autocorrelation function curve for *Cb. tepidum* chlorosomes having a hydrodynamic radius of 25.2 nm. The raw data was fit to the model shown in the inset of this plot. The model is described in Zander et al. (1996).

TABLE 1 Concentrations of chlorosomes and Bchl *c* along with determination of the amount of Bchl *c* per chlorosome w/(SD) values

OD 670	Bchl *c* (conc.)	Chlorosome (conc.)	R_h(DLS)	R_h(FCS)	Bchl *c*/chlorosome
42.1	$5.7 \times 10^{-4} \pm 7.0 \times 10^{-5}$ M	$2.6 \times 10^{-9} \pm 1.2 \times 10^{-9}$	26.8 ± 3.7 nm	25.2 ± 3.2 nm	215,000 ± 80,000

Final determinations of chlorosome Bchl *c* concentration as determined by pigment extraction, fluorescence correlation spectroscopy, and dynamic light scattering.

determined to contain 215,000 ± 80,000 Bchl *c* per chlorosome. The error is due to uncertainties in the dimensions of the probe volume of the single particle fluorescence apparatus.

DISCUSSION

The results presented in this study give the first direct determination of chlorosome pigment content. The findings of these studies indicate a surprisingly large number of Bchl *c* molecules present in a single chlorosome, 215,000 ± 80,000. As mentioned above, early estimates of Bchl *c* per chlorosome were on the order of 10,000 (Olson, 1998) although much debate has existed as to the validity of this number and the interpretation of aggregation models. Also, it must be noted that large variation in rod element organization between different species of green bacteria may be present, therefore causing a large amount of variation of pigment concentration between different species' chlorosomes.

To interpret these numbers, parameters from models proposed by the Holzwarth group were used (Holzwarth and Schaffner, 1994; Prokhorenko et al., 2000). Parameters for

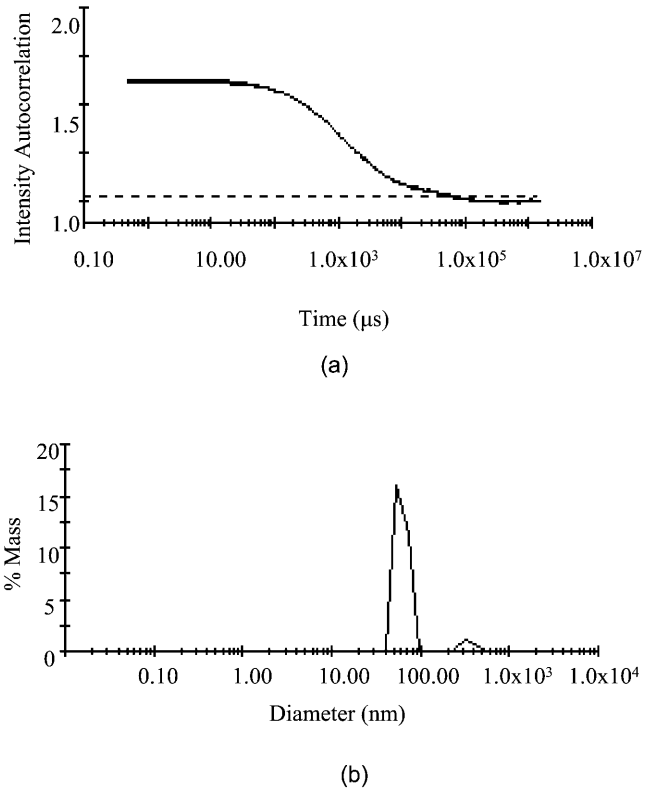

FIGURE 2 (*a*) Light-scattering autocorrelation function curve of chlorosomes. (*b*) The hydrodynamic radius of chlorosomes as determined by DLS using the Stokes-Einstein equation.

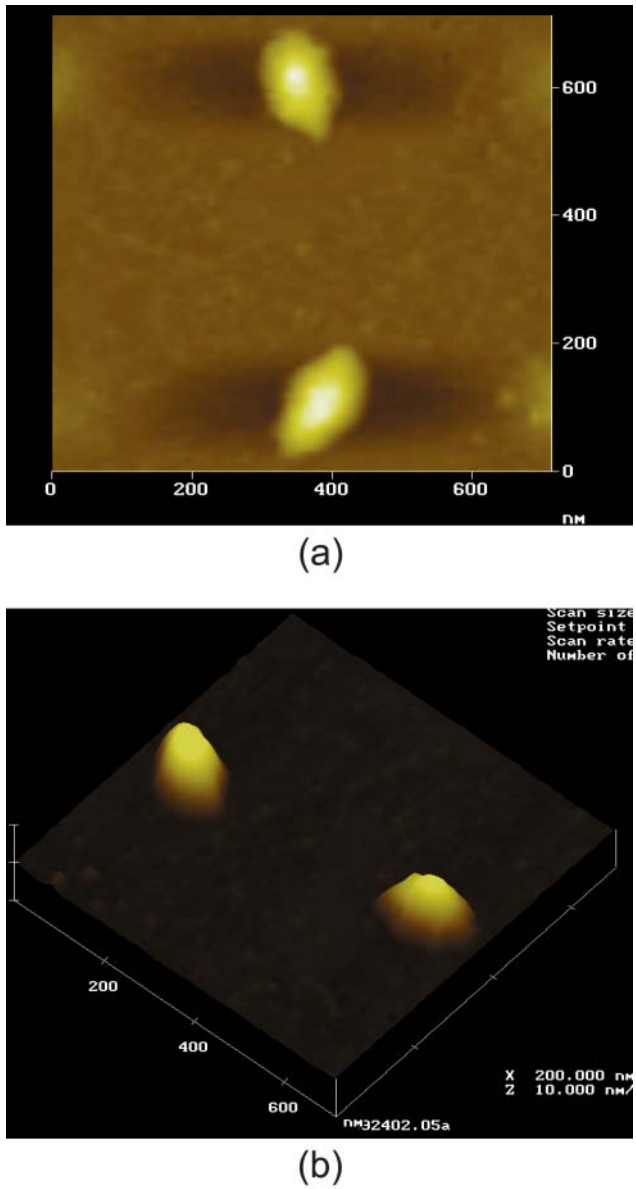

FIGURE 3 Tapping mode AFM image of *Cb. tepidum* chlorosomes adhered to mica surface. (*a*) Top view and (*b*) three-dimensional surface plot of chlorosomes with a scan size of 700 × 700 nm and a *Z* height range of 20 nm for *a* and 10 nm for *b*. Image taken in height mode.

TABLE 2 Parameters for chlorosome oligmer modeling

	Chloroflexus aurantiacus	*Chlorobium tepidum*
Diameter	45.94 Å	100 Å
Distance between chlorins in stacks (Mg-Mg atoms)	6.5 Å	6.5 Å
Stacks:Rod		36 (outer)
	18	4/6 outside:inside
TMAFM dimensions		174 ± 8.3 × 91.4 ± 7.7 × 10.86 ± 2.71 nm $n = 10$ (SD)
TMAFM volume		90,800 nm^3

Dimensions of rod element organization from Prokhorenko et al. (2000) and Van Rossum et al. (2002). TMAFM dimensions and volume determined from an average of 10 chlorosomes. TMAFM dimensions and volume determined from an average of 10 chlorosomes Dimensions used for chlorosome rod element modeling. Dimensions for chlorosomes and chlorosome volume determined from TMAFM.

Chlorobium-type chlorosomes are given and shown in Table 2. Using these values for rod element structure and the length of the chlorosomes obtained from our AFM studies, a number of ~16,000 Bchl *c* per rod element in the chlorosomes, used in this study, can be expected. This would indicate an average of 13.6 rod elements per chlorosome corresponding to 215,000 Bchl *c* per chlorosome for the volume measured per chlorosome by TMAFM.

Assuming a cylindrical rod element with volume $h\pi r^2$, and the same dimensions used above, 13.6 rod elements would have a volume of ~180,000 nm^3. The TMAFM pictures have an average volume of ~90,000 nm^3. However, it must be noted that AFM measurements of biological samples have given height measurements roughly half of what has been seen using electron microscopy (Butt et al., 1990; Eppell et al., 1993; Imai et al., 1993). Previous AFM measurements of chlorosomes also have been reported as being half of what has previously been observed by electron microscopy (Zhu et al., 1995). The heights reported by AFM in this study are on average about half of what would be expected for *Cb. tepidum* chlorosomes. The diameter for *Chlorobium*-type rod elements used in this study is ~10 nm. This would indicate a single layer of rod elements being present in each chlorosome. If it is assumed that the height of our chlorosomes is actually twice of that observed, this would give a volume for our chlorosomes of roughly 180,000 nm^3. This appears to be a likely scenario based on previous AFM evidence. Previous electron microscopy studies indicating multiple rod element layers per chlorosome would also indicate such a scenario (Staehelin et al., 1978, 1980). Extrapolating similar chlorosome dimensions and volumes from the obtained hydrodynamic radii is problematic. The hydrodynamic radii obtained are values based upon a spherical geometry that would induce the same friction with the solvent as the chlorosome. Therefore, Rh values should not be used for determining the volume of a chlorosome. Thus, the AFM measurements are determined to be best suited for any volume calculations.

As noted above, similar measurements on different species of chlorosomes may yield greatly different results. For instance, the model proposed for *Cf. aurantiacus* chlorosomes is that of a single layer of bacteriochlorophylls forming a rod element with half the diameter of the *Chlorobium*-type rod element. Applying the parameters for *Cf. aurantiacus* chlorosomes given by Prokhorenko et al. (2000) and van Rossum et al. (2001) and assuming the average dimensions reported for *Cf. aurantiacus* chlorosomes, (100 × 30 × 10 nm), ~40,000–60,000 Bchl *c* per chlorosome can be expected. However, these are only models and the actual rod element architecture may be different. Likewise, variation in growth conditions and environment also likely affects the overall pigment composition of the chlorosomes.

REFERENCES

Arellano, J. B., J. Psencik, C. M. Borrego, Y. Z. Ma, R. Guyoneaud, J. Garcia-Gil, and T. Gillbro. 2000. Effect of carotenoid biosynthesis inhibition on the chlorosome organization in *Chlorobium* phaeobacteroides strain CL1401. *Photochem. Photobiol.* 71:715–723.

Blankenship, R. E., J. M. Olson, and M. Miller. 1995. Antenna complexes from green photosynthetic bacteria. *In* Anoxygenic Photosynthetic Bacteria. R. E. Blankenship, M. T. Madigan, and C. E. Bauer, editors. Kluwer Academic Publishers, Dordrecht, The Netherlands. 399–435.

Brune, D. C., T. Nozawa, and R. E. Blankenship. 1987. Antenna organization in green Photosynthetic bacteria. 1. Oligomeric bacteriochlorophyll c as a model for the 740-nm absorbing bacteriochlorophyll-c in Chloroflexus aurantiacus chlorosomes. *Biochemistry.* 26:8644–8652.

Butt, H. J., K. H. Downing, and P. K. Hansma. 1990. Imaging the membrane-protein bacteriorhodopsin with the atomic force microscope. *Biophys. J.* 58:1473–1480.

Cohen-Bazire, G. N., N. Pfennig, and R. Kunisawa. 1964. The fine structure of green bacteria. *J. Cell Biol.* 22:207–225.

Ehrenber, M., and R. Rigler. 1974. Rotational brownian-motion and fluorescence intensity fluctuations. *Chem. Phys.* 4:390–401.

Eppell, S., F. Zypman, and R. Marchant. 1993. Probing the resolution limits and tip interactions of atomic-force microscopy in the study of globular-proteins. *Langmuir.* 9:2281–2288.

Feick, R. G., M. Fitzpatrick, and R. C. Fuller. 1982. Isolation and characterization of cytoplasmic membranes and chlorosomes from the green bacterium Chloroflexus aurantiacus. *J. Bacteriol.* 150:905–915.

Feick, R. G., and R. C. Fuller. 1984. Topography of the photosynthetic apparatus of *Choloroflexus aurantiacus. Biochemistry.* 23:3693–3700.

Fries, J., L. Brand, C. Eggeling, M. Kollner, and C. Seidel. 1998. Quantitative identification of different single molecules by selective time-resolved confocal fluorescence spectroscopy. *J. Phys. Chem. A.* 102:6601–6613.

Frigaard, N., S. Takaichi, M. Hirota, K. Shimada, and K. Matsuura. 1997. Quinones in chlorosomes of green sulfur bacteria and their role in the redox-dependent fluorescence studied in chlorosome-like bacteriochlorophyll c aggregates. *Arch. Microbiol.* 167:343–349.

Griebenow, K., and A. R. Holzwarth. 1989. Pigment organization and energy-transfer in green bacteria. 1. Isolation of native chlorosomes free of bound bacteriochlorophyll-a from Chloroflexus-aurantiacus by gel-electrophoretic filtration. *Biochim. Biophys. Acta.* 973:235–240.

Holzwarth, A. R., and K. Schaffner. 1994. On the structure of bacteriochlorophyll molecular aggregates in the chlorosomes of green bacteria—a molecular modeling study. *Photosynth. Res.* 41:225–233.

Imai, K., K. Yoshimura, M. Tomitori, O. Nishikawa, R. Kokawa, M. Yamamoto, M. Kobayashi, and A. Ikai. 1993. Scanning tunneling and

atomic-force microscopy of T4-bacteriophage and tobacco mosaic-virus. *Japanese Journal of Applied Physics Part 1-Regular Papers Short Notes & Review Papers*. 32:2962–2964.

Magde, D., W. Webb, and E. Elson. 1972. Thermodynamic fluctuations in a reacting system—measurement by fluorescence correlation spectroscopy. *Phys. Rev. Lett.* 29:705–708.

Martinez-Planells, A., J. B. Arellano, C. A. Borrego, C. Lopez-Iglesias, F. Gich, and J. S. Garcia-Gil. 2002. Determination of the topography and biometry of chlorosomes by atomic force microscopy. *Photosynth. Res.* 71:83–90.

Matsuura, K., M. Hirota, K. Shimada, and M. Mimuro. 1993. Spectral forms and orientation of bacteriochlorophyll-c and bacteriochlorophyll-a in chlorosomes of the green photosynthetic bacterium Chloroflexus-aurantiacus. *Photochem. Photobiol.* 57:92–97.

Nozawa, T., K. Ohtomo, M. Suzuki, Y. Morishita, and H. Konami. 1992a. Cp Mas C-13 NMR-studies on antenna structures in chlorosomes in green bacteria. *Photosynth. Res.* 34:112–112.

Nozawa, T., K. Ohtomo, N. Takeshita, Y. Morishita, M. Osawa, and M. T. Madigan. 1992b. Substituent effects on the aggregation of bacteriochlorophyll-d homologs purified from Chlorobium-limicola. *Bull. Chem. Soc. Jpn.* 65:3493–3494.

Oelze, J., and J. Golecki. 1995. Membranes and chlorosomes for green bacteria: structure, composition and development. *In* Anoxygenic Photosynthetic Bacteria. R. E. Blankenship, M. T. Madigan, and C. E. Bauer, editors. Kluwer Academic Publishers, Dordrecht, The Netherlands. 259–278.

Olson, J. M. 1998. Chlorophyll organization and function in green photosynthetic bacteria. *Photochem. Photobiol.* 67:61–75.

Prokhorenko, V. I., D. B. Steensgaard, and A. F. Holzwarth. 2000. Exciton dynamics in the chlorosomal antennae of the green bacteria Chloroflexus aurantiacus and Chlorobium tepidum. *Biophys. J.* 79:2105–2120.

Rigler, R., U. Mets, J. Widengren, and P. Kask. 1993. Fluorescence correlation spectroscopy with high count rate and low-background—analysis of translational diffusion. *Eur. Biophys. J.* 22:169–175.

Sprague, S. G., and L. A. Staehelin. 1984. Effects of reconstitution method on the structural organization of isolated chloroplast membrane-lipids. *Biochim. Biophys. Acta.* 777:306–322.

Staehelin, L. A., J. R. Golecki, and G. Drews. 1980. Supramolecular organization of chlorosomes (Chlorobium vesicles) and of their membrane attachment sites in Chlorobium-limicola. *Biochim. Biophys. Acta.* 589:30–45.

Staehelin, L. A., J. R. Golecki, R. C. Fuller, and G. Drews. 1978. Visualization of the supramolecular architecture of chlorosomes (Chlorobium type vesicles) in freeze-fractured cells of Chloroflexus-aurantiacus. *Arch. Microbiol.* 119:269–277.

Wahlund, T. M., C. R. Woese, R. W. Castenholz, and M. T. Madigan. 1991. A thermophilic green sulfur bacterium from New Zealand hot-springs, Chlorobium-tepidum Sp-Nov. *Arch. Microbiol.* 156:81–90.

Zander, C., M. Sauer, K. H. Drexhage, D. S. Ko, A. Schultz, J. Wolfrum, L. Brand, C. Eggeling, and C. A. M. Seidel. 1996. Detection and characterization of single molecules in aqueous solution. *Applied Physics B-Lasers and Optics.* 63:517–523.

Zhu, Y. W., B. L. Ramakrishna, P. I. vanNoort, and R. E. Blankenship. 1995. Microscopic and spectroscopic studies of untreated and hexanol-treated chlorosomes from Chloroflexus aurantiacus. *Biochimica Et Biophysica Acta-Bioenergetics.* 1232:197–207.